2,4-Di([1-^{13}C]-1-hydroxyethyl)deuteroporphyrin IX Dimethyl Ester (48). The foregoing carbon-13 enriched diacetylporphyrin (20 mg) in 50 mL of chloroform was treated with a solution of 20 mg of sodium borohydride in 2 mL of ice-cold methanol. The mixture was stirred at room temperature for 25 min, after which time it was determined by analytical TLC that reaction was complete. Spectrophotometry also showed a hypsochromic shift in the 639-nm band to 619 nm. Excess hydride was decomposed by addition of 150 mL of 0.04 M hydrochloric acid and the solution was then carefully neutralized with aqueuous ammonia. The organic layer was separated and evaporated to dryness to give a residue which was recrystallized from dichloromethane/hexane to give 18 mg (90%) of doubly labeled hematoporphyrin IX dimethyl ester (**48**), mp 219-220 °C (lit.[50] mp 223 °C). The carbon-13 NMR spectrum at 50 MHz showed a single enriched peak at 62.50 ppm which became a doublet in the proton-coupled mode, with J_{C-H} = 140.6 Hz.

2,4-Di([1-^{13}C]vinyl)deuteroporphyrin IX Dimethyl Ester (44). The carbon-13 enriched hematoporphyrin (**48**) (18 mg) was dissolved in 6 mL of dimethylformamide containing 1 mL of benzoyl chloride and heated at 90 °C for 1.5 h. After this time 2 mL of triethylamine was added to the warm solution, followed by 15 mL of water and 7 mL of methanol. The mixture was shaken to precipitate the product, which was collected by filtration through Celite, and then washed with 10 mL of water and redissolved by addition of 20 mL of chloroform and then collection by suction through the Celite. The organic phase was evaporated and the residue was purified by chromatography on 1-mm thick 20 × 20 cm preparative silica gel TLC plates (elution with 2% methanol in dichloromethane). The porphyrin was recovered from the silica by washing with 3% methanol in dichloromethane, and, after crystallization from dichloromethane/hexane, a quantitative yield of doubly labeled protoporphyrin IX dimethyl ester (**44**) was obtained, with mp 215-217 °C (lit.[50] mp 228-229 °C, unlabeled). The carbon-13 ^{1}H NMR spectrum showed a single enhanced peak at 130.32 ppm, and in the proton-coupled mode the J_{C-H} was 153.4 Hz: ^{1}H NMR δ (ppm) -3.70 (br s, 2 H, NH), 3.30 (m, 4 H, CH_2CO), 3.68, 3.69, 3.76, 3.77, 3.93 (each s, 3 H, 3 H, 3 H, 3 H, 6 H, Me, and OMe), 4.23, 4.43 (each m, 2 H, CH_2CH_2CO), 6.21, 6.41 each d, 2 H, $CH{=}CH_2$), 8.10, 8.52 (each m, 1 H, $CH{=}CH_2$), 10.05, 10.15, 10.21, 10.30 (each s, 1 H, meso H).

Typical Iron Insertion Procedure: Synthesis of Hemin Chloride Dimethyl Ester. To a three-necked, 100-mL round-bottom flask, equipped with a reflux condenser (topped with a nitrogen gas inlet), a pressure-equilibrated dropping funnel (topped with a septum cap), and a nitrogen gas escape tube (with a glycerol bubbler), was added 25 mL of acetonitrile. After refluxing the acetonitrile for 30 min with vigorous stirring (bar magnet) and under a stream of nitrogen, 150 mg of ferrous chloride hydrate was added, and this dissolved with the heat. The mixture was cooled to 50 °C and a solution of 110 mg of protoporphyrin IX dimethyl ester (**1**) in nitrogen-purged chloroform (12 mL) was transferred through the septum cap into the dropping funnel. Though some of the ferrous salt had precipitated, the porphyrin solution was added to the stirred ferrous chloride solution at a rate of 2 mL per min. After complete addition, the mixture was stirred for a further 10 min under nitrogen before being exposed to air. The resulting brown solution was then diluted with 125 mL of dichloromethane and washed with 125 mL of 0.2 M hydrochloric acid, and then with 100 mL of water. The organic phase was collected, the solvent evaporated, and the residue sampled by analytical silica gel TLC. The chromatogram indicated that no free base **1** was present and that no ester hydrolysis had occurred. The residue was chromatographed (optional) on neutral alumina (Brockmann Grade III, elution with chloroform containing 0.5% methanol). The major fraction was collected, washed with 0.1 M hydrochloric acid, and then evaporated to dryness to give a brown residue which was crystallized from dichloromethane/heptane to give hemin chloride dimethyl ester (116 mg, 92%), identical by TLC and ^{1}H NMR spectroscopy (as the cyanoferrihemin) with an authentic sample.

Typical Ester Hydrolysis: Synthesis of Hemin (5). The foregoing hemin dimethyl ester (50 mg) was dissolved in 15 mL of a solution made by mixing 95 mL of methanol, 5 mL of water, and 1 g of potassium hydroxide. The solution was refluxed for 5 h at 60 °C under an atmosphere of dry nitrogen. The warm solution was then diluted with 20 mL of methylene chloride and washed with 2 × 50 mL of 0.2 M hydrochloric acid. The organic phase was collected, dried (Na_2SO_4), and evaporated to dryness to give a residue which was recrystallized from tetrahydrofuran to give 40 mg (80% yield) of hemin, identical with an authentic sample by TLC, spectrophotometry, and ^{1}H NMR spectroscopy (in D_2O, as the dicyanohemin).

Acknowledgment. This research was supported by grants from the National Institutes of Health (HL 22252) and the National Science Foundation (CHE-78-25557). We are pleased to acknowledge financial asistance (to H.D.T.) from Yarmouk University, Jordan.

Registry No. 1, 5522-66-7; **2**, 10591-31-8; **3**, 13003-76-4; **4**, 15295-25-7; **5**, 16009-13-5; **8**, 14376-24-0; **10**, 74822-24-5; **11**, 74822-25-6; **12**, 63148-21-0; **13**, 18210-87-2; **14**, 87191-13-7; **15**, 87191-14-8; **16**, 52459-76-4; **17**, 52459-74-2; **21**, 87206-75-5; **23**, 87191-08-0; **23** acetyl derivative, 87206-74-4; **24**, 87191-15-9; **24** dimethyl ketal derivative, 87191-19-3; **25**, 87191-17-1; **25** undeuterated, 58684-37-0; **25** dimethyl ketal derivative, 87191-16-0; **26**, 87191-20-6; **26** undeuterated, 87191-18-2; **27**, 87206-76-6; **27** undeuterated, 58684-43-8; **28**, 10200-04-1; **28** zinc complex, 61577-42-2; **29**, 15295-26-8; **30**, 17467-73-1; **31**, 52459-75-3; **32**, 87191-09-1; **33**, 52459-77-5; **33** copper complex, 87191-11-5; **34**, 87191-12-6; **35**, 52459-79-7; **36**, 87206-77-7; **37**, 87191-21-7; **38**, 87191-22-8; w39, 13187-15-0; **40**, 15341-25-0; **40** zinc complex, 87191-10-4; **41**, 5522-66-7; **42**, 87191-23-9; **43**, 87226-18-4; **44**, 87191-26-2; **45**, 87191-24-0; **46**, 87206-79-9; **47**, 87206-78-8; **48**, 87191-25-1; deuterohemin dimethyl ether, 19442-32-1; sodium [1-^{13}C]acetate, 23424-28-4; hemin chloride dimethyl ester, 15741-03-4.

Ab Initio Investigation on the Lowest Singlet and Triplet State of Si_2H_2

Hans Lischka*[†] and Hans-Joachim Köhler[‡]

Contribution from the Institut für Theoretische Chemie und Strahlenchemie, Universität Wien, A-1090 Wien, Austria, and Organisations- und Rechenzentrum der Karl Marx Universität Leipzig, DDR-7010 Leipzig, German Democratic Republic. *Received February 28, 1983*

Abstract: Ab initio SCF and electron correlation calculations are reported for the Si_2H_2 system. In the case of the singlet ground state the global minimum is a nonplanar bridged structure (IV) followed by H_2SiSi (II) and trans-bent HSiSiH (I). Both H_2SiSi and trans-bent HSiSiH are predicted to be local minima. Stability differences ($\Delta H°_{298.16}$) obtained from our most extensive calculations are II/IV 11.8 kcal/mol and I/IV 14.3 kal/mol. In the triplet case H_2SiSi (II) is the global minimum. Trans bent HSiSiH (I) and a planar bridged structure (III) are local minima. The following stability differences were obtained: I/II 1.7 kcal/mol, III/II 19.7 kcal/mol.

1. Introduction

Compounds containing silicon involved in multiple bonds have always attracted the interest of theoretical and experimental chemists. However, despite the numerous experimental investigations, direct structural evidence thereof is rather scarce. In recent years theoretical methods have been developed to a degree which allows in many cases (especially for closed-shell ground states) the accurate prediction of structures and stability differences. In the case of silaolefins the interrelation between theory

[†] Universität Wien.
[‡] Karl Marx Universität.

0002-7863/83/1505-6646$01.50/0

Chart I

basis set no.	
1	Si: 10s6p1d (0.4) H: 3s
2	Si: 11s7p1d (0.4) H: 4s
3	Si: 11s7p1d (0.4) H: 4s1p (0.4)
4	Si: 11s7p2d (0.2, 0.7) H: 4s1p (0.4)

and experiment has been nicely reviewed by Schaefer.[1] We refer to his paper for a documentation of recent experimental and theoretical work on this topic.

The question whether silicon–silicon double and triple bonds exist is of principal interest in chemistry. For example, Si_2H_4 has been detected in the pyrolysis products of silicon hydrides.[2] However, whether the observed species was disilene (H_2SiSiH_2) or silylsilylene ($HSiSiH_3$) remained unclear. Only in the past few years have stable disilene compounds been prepared.[3a,b] A series of theoretical calculations has been performed on the Si_2H_4 system as well.[4-11] Two local minima have been observed, one corresponding to $HSiSiH_3$ and the other to H_2SiSiH_2, the latter structure probably being somewhat more stable than the former one. The two minima are separated by a barrier of about 17 kcal/mol.[10]

The Si_2H_2 system is of interest because it can act as a model for Si/Si triple bonds. To our knowledge no experimental information on Si_2H_2 is available. Several theoretical calculations have been published so far.[4,12-15] It turns out that for the description of structures and relative stabilities smaller basis sets are not adequate and that also electron correlation effects are crucial. As we shall show, our results and conclusions differ considerably from the previously published investigations. However, after completion of our calculations we acquired knowledge of unpublished work of the groups of Pople and Schleyer[16] and of Morokuma[17] which goes at least in part very much along the lines of our results.

2. Computational Details

For a complete description of the computational procedures employed here we refer to our previous work.[11] The Huzinaga basis sets[18] are given in Chart I together with the exponents for the polarization functions.

The 10s6p set was contracted to (511111/3111), the 11s7p set to (5111111/31111), the 3s set to (21), and the 4s set to (211). A scaling factor of 1.44 was used for the s functions on hydrogen. The geometries were optimized at the SCF level and with inclusion of electron correlation by CEPA-2[19] using basis set 1. The stationary points were characterized by the matrix of force constants. This was done in a complete way at the SCF level. Within the CEPA approach a complete determination of the harmonic force field has been performed only for the most stable, bridged singlet structure and only a partial evaluation for the other structures.

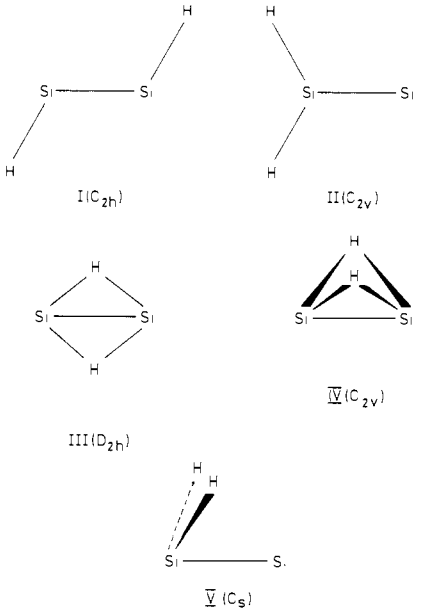

Figure 1. The structures investigated in this work.

Table I. SCF and CEPA Geometries for the Singlet and Triplet State[a]

	singlet		triplet	
	SCF	CEPA	SCF	CEPA
structure I				
R_{SiSi}	2.090	2.152	2.321	2.339
R_{SiH}	1.492	1.510	1.512	1.528
∠SiSiH	126.3	122.4	104.3	104.0
structure II				
R_{SiSi}	2.197	2.256	2.311	2.325
R_{SiH}	1.487	1.501	1.491	1.507
∠HSiH	111.5	111.9	106.6	106.1
structure III				
R_{SiSi}	2.384	2.479	2.772	2.761
R_{SiH}	1.607	1.644	1.729	1.733
structure IV				
R_{SiSi}	2.216	2.246		
R_{SiH}	1.724	1.732		
∠HSiH	71.4	71.9		
structure V				
R_{SiSi}		2.260		
R_{SiH}		1.534		
∠HSiH		84.6		
∠HSiSi		100.9		

[a] Bond distances are given in Å; angles are given in degrees.

3. Results and Discussions

3.1. The Singlet State. The most extensive calculation published so far is the one by Snyder et al.[15] using pseudopotential single-ζ SCF and GVB techniques. A series of structures have been

(1) Schaefer, H. F., III *Acc. Chem. Res.* **1982**, *15*, 283.
(2) Sefcik, M. D.; Ring, M. B. *J. Am. Chem. Soc.* **1973**, *95*, 5168.
(3) (a) West, R.; Fink, M. J. *Science* **1981**, *214*, 1343. (b) Masamune, S.; Hanzawa, Y.; Murakami, Sh.; Bally, Th.; Blount, J. R. *J. Am. Chem. Soc.* **1982**, *104*, 1150.
(4) Blustin, H. P. *J. Organomet. Chem.* **1976**, *105*, 161.
(5) Daudel, R.; Kari, R. E.; Poirier, R. A.; Goddard, J. D.; Csizmadia, I. G. *J. Mol. Struct.* **1978**, *50*, 115.
(6) Roeland, F. F.; van de Vondel, D. F.; van der Kelen, G. P. *J. Organomet. Chem.* **1979**, *165*, 151.
(7) Snyder, L. C.; Wasserman, Z. R. *J. Am. Chem. Soc.* **1979**, *101*, 5222.
(8) Poirier, R. A.; Goddard, J. D. *Chem. Phys. Lett.* **1981**, *80*, 37.
(9) Krogh-Jespersen, K. *J. Phys. Chem.* **1982**, *86*, 1492.
(10) Krogh-Jespersen, K. *Chem. Phys. Lett.* **1982**, *93*, 327.
(11) (a) Lischka, H.; Köhler, H. J. *Chem. Phys. Lett.* **1982**, *85*, 467. (b) Köhler, H. J.; Lischka, H. *J. Am. Chem. Soc.* **1982**, *104*, 5884.
(12) Wirsam, B. *Theor. Chem. Acta* **1972**, *25*, 169.
(13) Obara, Sh.; Kitaura, K.; Morokuma, K. *Theor. Chim. Acta* **1981**, *60*, 227.
(14) Kawai, F.; Noro, T.; Murakami, A.; Ohno, K. *Chem. Phys. Lett.* **1982**, *92*, 479.
(15) Snyder, L. C.; Wasserman, Z. R.; Moskowitz, J. W. *Int. J. Quantum Chem.* **1982**, *XXI*, 565.
(16) Luke, B. T.; Pople, J. A.; Krogh-Jespersen, M. B.; Apeloig, Y.; Chandrasekhar, J.; Schleyer, P. v. R., private communication.
(17) Hanamura, M.; Morokuma, K.; Nagase, Sh. Institute for Molecular Science, 1980.
(18) Huzinaga, S. Approximate Atomic Functions I and II, University of Alberta, Canada, 1971.
(19) (a) Meyer, W. *Int. J. Quantum. Chem.* **1971**, *S5*, 341. (b) Meyer, W. *J. Chem. Phys.* **1973**, *58*, 1017. (c) Meyer, W. *Theor. Chim. Acta*, **1974**, *35*, 277.

Table II. Total Energies (au) and Zero Point Energies (kcal/mol)

	$-E_{SCF}$				$-E_{CEPA}$				
	basis set 1	basis set 2	basis set 3	basis set 4	basis set 1	basis set 2	basis set 3	basis set 4	ϵ_0
structure I									
^1A_g	578.63948	578.83749	578.84115	578.84539	578.85580	579.07141	579.09272	579.10737	8.0
^3A_u	578.66528	578.86000	578.86359	578.86897	578.84528	579.05673	579.08018	579.09579	8.5
structure II									
$^1A_1$	578.67242	578.86959	578.87290	578.87968	578.86321	579.07611	579.09747	579.11478	9.7
$^3A_2$	578.68348	578.87840	578.88167	578.88867	578.84902	579.06060	579.08248	579.10081	9.7
structure III									
^1A_g	578.64479	578.83922	578.85174	578.85774	578.85644	579.06728	579.10173	579.11723	10.0
$^3B_{3u}$	578.64364	578.82958	578.83915	578.84111	578.81278	579.01630	579.05186	579.06695	8.5
structure IV									
$^1A_1$	578.68692	578.87435	578.88474	578.88892	578.87882	579.08534	579.11878	579.13229	9.4
structure V									
$^1A'$	578.65033	578.84108	578.84603	578.85193	578.84578	579.05424	579.07897	579.09625	

Table III. Relative Stabilities for the Singlet-State Structures[a]

	ΔE_{SCF}				ΔE_{CEPA}				
	basis set 1	basis set 2	basis set 3	basis set 4	basis set 1	basis set 2	basis set 3	basis set 4	$\Delta H^\circ_{298.16}$
structure I	29.8	23.1	27.4	27.3	14.4	8.7	16.4	15.6	14.3
structure II	9.1	3.6	7.4	5.8	9.8	5.8	13.4	11.0	11.8
structure III	26.4	22.1	20.7	19.6	14.0	11.3	10.7	9.5	
structure IV	0	0	0	0	0	0	0	0	0
structure V	23.0	20.9	24.3	23.2	20.7	19.5	25.0	22.6	

[a] Energies are given in kcal/mol.

Table IV. Harmonic Vibrational Frequencies (cm^{-1}) Calculated with Basis Set 1

singlet states					triplet states			
structure II		structure IV			structure II		structure III	
SCF		SCF	CEPA		SCF		SCF	
a_1	2257	a_1	1577	1514	a_1	2244	a_g	1580
	970		1070	958		1044		406
	561		583	517		453	b_{1g}	1013
b_1	422	a_2	795	735	b_1	382	b_{1u}	345
b_2	2270	b_1	1018	940	b_2	2241	b_{2u}	1144
	319	b_2	1517	1425		453	b_{3u}	1314

Table V. SiSi Force Constants (mdyn/Å) Obtained at the CEPA Level (Basis Set 1)

structure	K_{SiSi}
singlet state	
I	2.25
II	1.92
III	1.38
IV	2.37
triplet state	
I	1.54
II	1.61
III	1.29

investigated very similar to the ones we are considering. In the other previous calculations,[12-14] only a rather restricted choice of structures is treated.

In Figure 1 the geometries investigated in this work are depicted. Table I shows the geometry parameters resulting both from SCF and CEPA computations. In addition, we also calculated in preliminary investigations the linear structure of disilyne. However, it turned out to be a stationary point with two negative eigenvalues in the force constant matrix. Since linear disilyne was also energetically very unfavorable, we removed it from our list of structures of interest.

A twisted dihedral form of disilyne is reported by Kawai et al.[14] as well as by Snyder et al.[15] Both groups used only single-ζ or double-ζ basis sets for geometry optimization. However, using more flexible basis sets, especially with inclusion of d-functions, changes the situation completely. Starting from the dihedral structure the energy decreases gradually upon reducing the HSiSi angle and one ends up in the bridged structure IV of Figure 1. This behavior has also been observed in ref 16. Thus, we do not think that twisted dihedral disilyne is a structure which corresponds to a local minimum.

Comparing the SiSi bond distance in trans-bent disilyne (structure I) with R_{SiSi} in disilene (2.17 Å from our CEPA cal-

Table VI. Relative Stabilities for the Triplet-State Structures[a]

	ΔE_{SCF}				ΔE_{CEPA}				
	basis set 1	basis set 2	basis set 3	basis set 4	basis set 1	basis set 2	basis set 3	basis set 4	$\Delta H^\circ_{298.16}$
structure I	11.4	11.5	11.3	12.4	2.3	2.4	1.4	3.2	1.7
structure II	0	0	0	0	0	0	0	0	0
structure III	25.0	30.6	26.7	29.9	22.7	27.8	19.2	21.3	19.7

[a] Energies are given in kcal/mol.

Table VII. Singlet-Triplet Splittings (kcal/mol)[a]

	ΔE_{SCF}				ΔE_{CEPA}				
	basis set 1	basis set 2	basis set 3	basis set 4	basis set 1	basis set 2	basis set 3	basis set 4	$\Delta H^\circ_{298.16}$
structure I	−16.2	−14.1	−14.1	−14.8	6.6	9.2	7.9	7.3	7.9
structure II	−6.9	−5.5	−5.5	−5.6	8.9	9.7	9.4	8.8	8.8
structure III (triplet)/ structure IV (singlet)	27.2	28.1	28.6	30.0	41.5	43.3	42.0	41.0	40.2

[a] A positive sign implies that the singlet state is more stable than the triplet state.

culation in ref 11) one can see that they are almost the same. In the other structures of Si_2H_2 R_{SiSi} is even longer.

In Tables II and III total energies and relative stabilities are collected. The order in stabilities and the numerical values differ significantly from those in ref 15. In contrast to Snyder et al.,[15] we find that the bridged disilyne (IV) is the global minimum. We attribute the discrepancies to the much smaller basis sets used in their calculations. On the other hand, our findings are in agreement with the unpublished works of ref 16 and 17.

The disilenylidene structure (II) is a local minimum about 11 kcal/mol above the bridged structure IV. Structure IV is separated from II by a barrier of ~23 kcal/mol. The planar bridged structure III is a saddle point for the interconversion of structure IV into the equivalent form IV′.

For structures II–V the general feature whether a structure is a minimum or a saddle point is the same at the SCF and CEPA levels. In the case of trans-bent disilyne (I) the situation is more complicated. The SCF calculations with basis set 1 show two negative eigenvalues in the harmonic analysis. One corresponds to the HSiSiH torsional motion and the other to a motion which is dominated by the antisymmetric combination of the HSiSi and SiSiH angles. As one can see from Table III trans-bent disilyne gains in stability by including electron correlation effects. Thus one could suspect that structure I might be a local minimum as well. We computed at the CEPA level the torsional and the antisymmetric bending motion and found indeed that the system was stable with respect to the pertaining displacements. In this approach the coupling between the antisymmetric bending and the antisymmetric SiH stretching modes has been neglected. Since this coupling is rather small we do not expect any influence on qualitative features. We therefore conclude that trans-bent disilyne is a local minimum.

In Table IV the harmonic vibrational frequencies for disilenylidene (II) and bridged disilyne (IV) are reported. In the latter case the complete harmonic force field was also obtained using the CEPA approach. Table V shows for comparison the SiSi stretching force constants.

3.2. The Triplet State. Our results for the lowest triplet state are shown in Tables II and IV–VII. The most stable structure is disilenylidene (II). The planar bridged structure III is found to be a local minimum as well, even though it is about 20 kcal/mol above II. As in the singlet case a significant stabilization of the trans-bent form (I) relative to II is observed. At the SCF level we find for structure I one negative eigenvalue in the force constant matrix corresponding to the antisymmetric in plane bending motion. Proceeding in the same way as before, we recalculated the antisymmetric bending motion by means of CEPA and again found that the energy was stable toward respective displacements.[20] Therefore, triplet trans-bent disilyne is a local minimum as well.

Table VII shows singlet/triplet splittings for corresponding structures. It is interesting to note that at the SCF level the triplet states of structures I and II are lower in energy than the corresponding singlet states. However, inclusion of electron correlation puts the triplet states above the singlets.

4. Conclusions

Our results show that only large-scale calculations including electron correlation effects can give a correct picture of the structure and stability of the Si_2H_2 system. Even though in the singlet state the bridged structure is clearly the most stable one, disilenylidene and bent disilyne are still close in energy so that they cannot be omitted in further discussions. In particular, there are two questions which come to mind if one considers the present situation: (a) are there any stable bridged structures also in other cases (like Si_2H_4), and (b) what happens if the bridging hydrogen atoms are replaced by bulkier groups? Investigations along these lines are being carried out in our group at present.

Acknowledgment. This work was carried out under the auspices of the WTZ-treaty between Austria and the German Democratic Republic. The calculations were performed on the CDC CYBER 170-720 computers of the IEZ Vienna.

Registry No. Disilyne, 36835-58-2.

(20) In the case of the antisymmetric bending coordinate $\Delta\alpha = \angle$HSiSi−$\angle$SiSiH a discontinuity was observed for the energy curve at $\Delta\alpha = 0$ (i.e., for the C_{2h} structure). This discontinuity occurred at the SCF level as well as on the CI and CEPA levels. We circumvented this problem by excluding the point $\Delta\alpha = 0$. Instead, we performed an extrapolation for $\Delta\alpha \rightarrow 0$ from points situated closely enough to $\Delta\alpha = 0$.